To appear in Grazer Math. Berichte (2002)

EFFICIENT SIMULATION TECHNIQUES FOR A GENERALIZED RUIN MODEL*

HANSJÖRG ALBRECHER REINHOLD KAINHOFER ROBERT F. TICHY

Abstract

In this paper we consider a generalized version of the classical model for the collective surplus process of an insurance portfolio. In the presence of dividend payments according to a non-linear barrier strategy and interest on the free reserve we derive equations for the probability of ruin and the expected present value of dividend payments which give rise to several numerical number-theoretic solution techniques. For various claim size distributions and a parabolic barrier numerical tests and comparisons of these techniques are performed. In particular, the efficiency gain obtained by implementing low-discrepancy sequences instead of pseudorandom sequences is investigated.

1 Introduction

Let $\{N(t) : t \in \mathbb{R}_+\}$ denote the random process that counts the claims of an insurance portfolio of a company up to time t and assume that $N(t)$ is a homogeneous Poisson process with intensity λ. Let further $\{X_n : n \in \mathbb{N}\}$ be a sequence of independent identically distributed positive random variables with distribution function $F(y)$ representing the sizes of the successive claims and let $\mu = E(X_i) < \infty$. In a time interval $[t, t+dt]$ the company receives the premium $c\,dt$, where $c > \lambda \int_0^\infty y\,dF(y)$. In addition to the premium income, we assume that the company also receives interest on its reserves with a constant interest force i (for $i = 0$ we have the classical ruin model; for a general background in ruin theory see for instance GERBER [16], THORIN [26] or more recently DEVYLDER [10] and ASMUSSEN [5]). Let $T_n\,(n \in \mathbb{N})$ denote the moment of occurrence of the nth claim. If we introduce the purely discontinuous measure $X_{N_t}\,\mathrm{d}N_t$ which puts a weight equal to X_{N_t} at times $T_n\,(n \in \mathbb{N})$, then the value of the reserve at time t, denoted by R_t, satisfies

$$\mathrm{d}R_t = c\,\mathrm{d}t + R_t \cdot i\,\mathrm{d}t - X_{N_t}\,\mathrm{d}N_t$$

*This research was supported by the Austrian Science Fund Project S-8308-MAT

2000 Mathematics Subject Classification. Primary 62P05; Secondary 91B30

Key words and phrases. Cramer-Lundberg risk model, dividend barrier strategies, Quasi-Monte Carlo techniques, integro-differential equations

(see for example DELBAEN AND HAEZENDONCK [11]).
We now extend this model by introducing a time-dependent dividend barrier b_t, such that whenever the value of the reserve R_t reaches b_t, dividends are paid out to the shareholders with intensity $(c + R_t \cdot i) - db_t$ and the surplus remains on the barrier, until the next claim occurs. This means that the risk process develops according to

$$dR_t = (c + i\,R_t)\,dt - X_{N_t}\,\mathrm{d}N_t \qquad \text{if } R_t < b_t \tag{1}$$

$$dR_t = db_t - X_{N_t}\,\mathrm{d}N_t \qquad \text{if } R_t = b_t. \tag{2}$$

Together with the initial capital $R_0 = u,\ 0 \leq u < b_0 < \infty$, this determines the risk process $\{R_t,\ t \geq 0\}$ (cf. Figure 1).

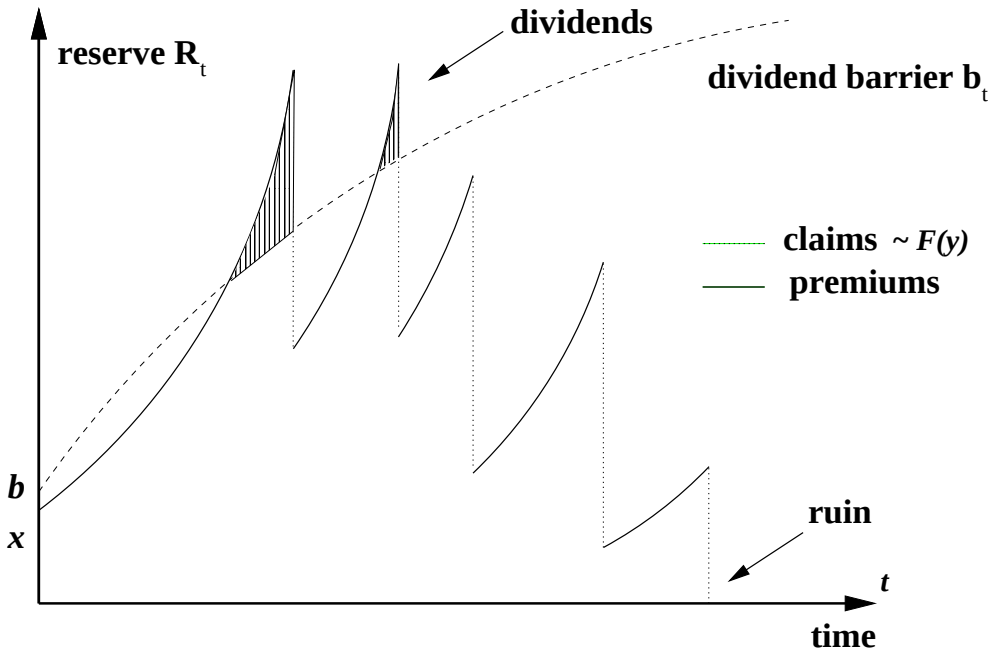

Figure 1: A sample path of R_t

The following quantities are of particular interest in this context: The survival probability is defined as the probability that the reserve of the portfolio never becomes negative, i.e.

$$\phi(u, b) = Pr\{R_t \geq 0\ \forall\ t \geq 0 \,|\, R_0 = u\},$$

where $u \geq 0$ denotes the initial reserve of the portfolio. Correspondingly the probability of ruin is defined by $\psi(u, b) = 1 - \phi(u, b)$. Another important quantity is the expected sum of discounted dividend payments $W(u, b)$, i.e. the expected present value of all dividends paid until ruin occurs.

Dividend barrier models have a long history in risk theory (see e.g. [8], [16]). GERBER [15] showed that barrier dividends constitute a complete family of Pareto-optimal

dividends. In the case of a horizontal dividend barrier $b_t \equiv b_c = \text{const.}$, we have $\phi(u,b) = 0 \; \forall \; 0 \leq u \leq b$. Including a constant interest force on the reserve in the model, PAULSEN AND GJESSING [21] calculated the optimal value of b_c that maximizes the expected value of the discounted dividend payments in this situation. For linear dividend barriers $b_t = b + at$ GERBER [14] derived an upper bound for the probability of ruin by martingale methods and in [17] he obtained exact solutions for the probability of ruin and the expected sum of discounted dividend payments $W(u,b)$ for exponentially distributed claim amounts; this result was generalized by SIEGL AND TICHY [24] to arbitrary Erlang claim amount distributions, see also ALBRECHER AND TICHY [4].

In [2] non-linear dividend barrier models of the type

$$b_t = \left(b^m + \frac{t}{\alpha} \right)^{1/m} \qquad (\alpha, b > 0, m \geq 1). \tag{3}$$

were introduced and integro-differential equations for $\phi(u,b)$ and $W(u,b)$ were derived. The existence and uniqueness of the corresponding solutions was discussed and techniques for numerical solutions were developed and tested for the case of an exponential claim size distribution. In [3] this approach was applied to more general claim size distributions and at the same time continuously compounded interest on the free reserve was included in the model.

This paper is a more general and extended version of [3]. In Section 2 we identify $\phi(u,b)$ and $W(u,b)$ as solutions of boundary value problems for integro-differential equations and also as fixed points of contracting integral operators which gives rise to the development of efficient number-theoretic simulation techniques based on Monte Carlo and Quasi-Monte Carlo methods. These are discussed in Section 3. In Section 4 we give detailed numerical results for a parabolic dividend barrier. The various simulation techniques are compared on a quantitative and qualitative basis. Finally the efficiency gain obtained by implementing various low-discrepancy sequences is investigated and the sensitivity of the simulation results with respect to the model assumptions is discussed.

2 Integro-differential equations and integral operators

In the sequel we will consider dividend barriers of type (3). Note that $m = 1$ corresponds to the linear barrier case.
The probability of survival $\phi(u,b)$ for the surplus process given by (1) and (2) can then be expressed as the solution of a boundary value problem in the following way:

Conditioning on the occurrence of the first claim, we get for $u < b$

$$\phi(u,b) = (1-\lambda dt)\phi\left(u + (c + i\,u)\,dt, \left(b^m + \frac{dt}{\alpha}\right)^{1/m}\right) + \\ + \lambda\,dt \int_0^{u+(c+i\,u)\,dt} \phi\left(u + (c+i\,u)\,dt - z, \left(b^m + \frac{dt}{\alpha}\right)^{1/m}\right) dF(z). \quad (4)$$

Taylor series expansion of (4) and division by dt shows that ϕ satisfies the equation

$$(c + i\,u)\,\frac{\partial \phi}{\partial u} + \frac{1}{\alpha\,m\,b^{m-1}}\,\frac{\partial \phi}{\partial b} - \lambda\,\phi + \lambda \int_0^u \phi(u-z,b)dF(z) = 0, \quad (5)$$

which, for reasons of continuity, is valid for $0 \le u \le b$. For $u = b$ the same arguments can be used to show that equation (5), with $c + i\,u$ replaced by $\frac{1}{\alpha m\,b^{m-1}}$, also holds. Thus we obtain the boundary condition

$$\frac{\partial \phi}{\partial u}\Big|_{u=b} = 0. \quad (6)$$

A further natural requirement is

$$\lim_{b\to\infty} \phi(u,b) = \phi(u), \quad (7)$$

where $\phi(u)$ is the probability of survival in absence of the barrier.

Let furthermore $W(u,b)$ denote the expected present value of the future dividend payments, which are discounted according to the riskless interest rate i, and stop when ruin occurs. Then, in a similar way to (4), one can derive the integro-differential equation

$$(c + i\,u)\,\frac{\partial W}{\partial u} + \frac{1}{\alpha\,m\,b^{m-1}}\,\frac{\partial W}{\partial b} - (i+\lambda)\,W + \lambda \int_0^u W(u-z,b)dF(z) = 0, \quad (8)$$

with boundary condition

$$\frac{\partial W}{\partial u}\Big|_{u=b} = 1. \quad (9)$$

Remark 1: In principle, one could follow this approach for any dividend barrier function $b_t = f(b,t)$ that is monotone increasing in t and satisfies

$$f(b,t) = f\Big(f(b,t_1), t - t_1\Big) \quad \forall\ b > 0 \text{ and } \forall\ t > t_1 > 0. \quad (10)$$

The functional equation (10) is the well-known translation equation and for functions $f(b,t)$ which are monotone increasing in b and t and continuous in b, the general solution of (10) is given by

$$f(b,t) = h\Big(h^{-1}(b) + t\Big),$$

where $h(t) = f(b_0, t)$ is some given initial function (see e.g. ACZÉL [1]). From $h(t) = (b_0^m + t/\alpha)^{\frac{1}{m}}$ we obtain (3) as a special case. Other solutions of (10) include for instance $f(b,t) = b + at$ (linear barrier) or $f(b,t) = (\sqrt{b} + t)^2$ (quadratic barrier).

Remark 2: For the special case of exponentially distributed claim sizes it follows from (5) and (8) that $\phi(u,b)$ and $W(u,b)$ can be expressed as the solutions of boundary value problems for second-order partial differential equations of hyperbolic type. However, due to the structure of the boundary conditions this does not lead to a simplification of the problem (cf. [2]).

Following a procedure developed by GERBER [17] for the case of linear barriers, we first show that the boundary value problem (8) together with (9) has a unique bounded solution. For that purpose, we define an operator A by

$$\begin{aligned} Ag(u,b) = &\int_0^{t^*} \lambda e^{-(\lambda+i)t} \int_0^{(c'+u)e^{it}-c'} g\left((c'+u)e^{it} - c' - z, \left(b^m + \frac{t}{\alpha}\right)^{1/m}\right) dF(z)dt + \\ &+ \int_{t^*}^{\infty} \lambda e^{-(\lambda+i)t} \int_0^{\left(b^m+\frac{t}{\alpha}\right)^{1/m}} g\left(\left(b^m + \frac{t}{\alpha}\right)^{1/m} - z, \left(b^m + \frac{t}{\alpha}\right)^{1/m}\right) dF(z)dt + \\ &+ \int_{t^*}^{\infty} \lambda e^{-\lambda t} \int_{t^*}^{t} e^{-is} \left((c + i\,u)e^{is} - \frac{1}{m\alpha\left(b^m + \frac{s}{\alpha}\right)^{1-1/m}}\right) ds\, dt, \quad (11) \end{aligned}$$

with $c' = c/i$. Here t^* is the positive solution of $(c'+u)e^{it} - c' = \left(b^m + \frac{t}{\alpha}\right)^{1/m}$ (this number is unique for all $m \geq 1$, since $u < b$). The solution $W(u,b)$ of (8) with its initial condition (9) is a fixed point of the integral operator A. For any two bounded functions g_1, g_2

$$|Ag_1(u,b) - Ag_2(u,b)| \leq \|g_1 - g_2\| \int_0^{\infty} \lambda e^{-(\lambda+i)t} dt \leq \frac{\lambda}{\lambda+i} \|g_1 - g_2\| \qquad (12)$$

for arbitrary $0 \leq u \leq b < \infty$, where $\|\cdot\|$ is the supremum norm on $0 \leq u \leq b < \infty$, and thus it follows that A is a contraction and the fixed point is unique by Banach's theorem.

The integral operator (11) does not only prove the existence and uniqueness of a solution of (8) and (9), but also allows for the development of numerical solution algorithms taking advantage of the contraction map (see Section 3).

Unfortunately, the same approach does not allow to show the contraction property of the corresponding integral operator for the probability of survival $\phi(u,b)$. We will see in Section 3, that by stochastic simulation of the risk reserve process one still can

obtain numerical solutions for $\phi(u,b)$ in a satisfying way. But especially for efficiency comparison purposes of the various numerical solution methods it would be nice to have such a contracting integral operator available. Thus we also consider a slight modification of our risk model in that we introduce an absorbing upper barrier $b_{max} \equiv const$, i.e. if the surplus process $R_t \geq b_{max}$ for some $t > 0$, it is absorbed, the dividend payments stop and the company is considered to have survived. From an economic point of view this can be interpreted that the company will then decide to pursue other forms of investment strategies. Mathematically, this model has some nice features (e.g. the process stops in finite time with probability 1). In the sequel we will refer to this modified version as Model B. The boundary value problem for the probability of survival can then be formulated by (5), (6) and

$$\phi(u, b_{max}) = \frac{\phi(u)}{\phi(b_{max})}, \tag{13}$$

where $0 \leq u \leq b \leq b_{max}$ and as before $\phi(u)$ is the probability of survival in absence of the barrier.

In Model B we can now proceed to obtain a contraction map for the probability of survival as its fixed point: Like in equation (11), let t^* be the time when the surplus would reach the dividend barrier given that no claim occurs. Let furthermore $t^{**} = \alpha(b_{max}^m - b^m)$ be the time when the dividend barrier reaches the absorbing barrier, and

$$\tilde{t} = \frac{1}{i} \log \left(\frac{c + i\, b_{max}}{c + i\, u} \right)$$

the time when the surplus would reach the absorbing barrier in the absence of a dividend barrier and of claims. As the dividend barrier is an increasing function on $\mathbb{R}^+$, t^{**} is uniquely determined, just as is $\tilde{t}$. Combining the two possible scenarios $0 \leq t^{**} \leq \tilde{t} \leq t^*$ and $0 \leq t^* \leq \tilde{t} \leq t^{**}$ (depending on the values of u and b), we define the operator A as

$$A\phi(u,b) = \int_0^T \lambda e^{-\lambda t} \int_0^{z_{max}(u,b,t)} \phi\left(z_{max}(u,b,t) - z, \left(b^m + \frac{t}{\alpha} \right)^{\frac{1}{m}} \right) dF(z)\, dt + e^{-\lambda T}, \tag{14}$$

where $T = \max\left(\tilde{t}, t^{**}\right)$ is the (finite) time when the surplus process reaches the absorbing upper barrier b_{max} in the absence of claims, and

$$z_{max}(u,b,t) = \min\left((c' + u)e^{it} - c', \left(b^m + \frac{t}{\alpha} \right)^{\frac{1}{m}} \right). \tag{15}$$

Let ϕ_1 and ϕ_2 now be two bounded functions on $0 \leq u \leq b \leq b_{max}$, then

$$|A\phi_1(u,b) - A\phi_2(u,b)| \leq \|\phi_1 - \phi_2\| \int_0^T \lambda e^{-\lambda t} dt = \|\phi_1 - \phi_2\| \left(1 - e^{-\lambda T}\right).$$

Since $T = T(u,b) < M < \infty$, this operator is a contraction, and Banach's fixed point theorem establishes the existence and uniqueness of the solution $\phi(u,b)$ in Model B.

Correspondingly, the contraction map for the expected sum of dividend payments in Model B is given by

$$\begin{aligned} Ag(u,b) = &\int_0^{t^*} \lambda e^{-(\lambda+i)t} \int_0^{(c'+u)e^{it}-c'} g\left((c'+u)e^{it}-c'-z, \left(b^m+\frac{t}{\alpha}\right)^{1/m}\right) dF(z)dt + \\ &+ \int_{t^*}^{t^{**}} \lambda e^{-(\lambda+i)t} \int_0^{\left(b^m+\frac{t}{\alpha}\right)^{1/m}} g\left(\left(b^m+\frac{t}{\alpha}\right)^{1/m} - z, \left(b^m+\frac{t}{\alpha}\right)^{1/m}\right) dF(z)dt + \\ &+ \int_{t^*}^{t^{**}} e^{-(\lambda+i)t}\left((c+i\,u)e^{it} - \frac{1}{m\alpha\left(b^m+\frac{t}{\alpha}\right)^{1-1/m}}\right) dt, \quad (16) \end{aligned}$$

if $t^{**} > t^*$ and $Ag(u,b) = 0$ otherwise, because then the surplus reaches the absorbing barrier before the dividend barrier. The last term in (16) represents the dividends that are paid out until t^{**} and is a simplification of the original expression

$$\begin{aligned} &\int_{t^*}^{t^{**}} \lambda e^{-\lambda t} \int_{t^*}^{t} e^{-is}\left((c+i\,u)e^{it} - \frac{1}{m\alpha\left(b^m+\frac{s}{\alpha}\right)^{1-1/m}}\right) ds\, dt + \\ &\qquad \int_{t^{**}}^{\infty} \lambda e^{-\lambda t} \int_{t^*}^{t^{**}} e^{-is}\left((c+i\,u)e^{it} - \frac{1}{m\alpha\left(b^m+\frac{s}{\alpha}\right)^{1-1/m}}\right) ds\, dt. \end{aligned}$$

From (16) it follows that

$$\|Ag_1(u,b) - Ag_2(u,b)\| \le \frac{\lambda}{\lambda+i}\left(1 - e^{-(\lambda+i)t^{**}}\right)\|g_1 - g_2\|\ ,$$

for any two bounded functions g_1, g_2 and we again have a contraction in the Banach space of bounded functions equipped with the supremum norm, which implies the existence and uniqueness of the solution.

Since these boundary value problems can not be solved analytically, there is a need for effective algorithms to obtain numerical solutions. In this paper we focus on the development of number-theoretic solution methods based on the corresponding integral operators and on stochastic simulation, respectively.

3 Numerical solution techniques

The following three algorithms are presented in terms of operator (11). However, the adaptation to the other integral operators introduced above is straight-forward.

3.1 Double-recursive Algorithm

Following a technique that was already used in TICHY [27], the fixed point of (11) can be approximated by applying the contracting integral operator A k times to a starting function $h(u,b)$ which we choose to be the inhomogeneous term in the corresponding integral operator (where k is chosen according to the desired accuracy of the solution):

$$g^{(k)}(u,b) = A^k g^{(0)}(u,b),$$
$$g^{(0)}(u,b) = h(u,b) := \int_{t^*}^{\infty} \lambda e^{-\lambda t} \int_{t^*}^{t} e^{-is} \left((c + i\,u) e^{is} - \frac{1}{m\alpha \left(b^m + \frac{s}{\alpha}\right)^{1-1/m}} \right) ds\, dt.$$

This leads to a $2k$-dimensional integral for $g^{(k)}(u,b)$, which is calculated numerically using Monte Carlo and Quasi-Monte Carlo methods. For that purpose we transform the integration domain of operator (11) into the unit cube:

$$Ag(u,b) = h(u,b) + \frac{\lambda}{\lambda+i} \cdot$$
$$\cdot \left[\left(1 - e^{-(\lambda+i)t^*}\right) \int_0^1 \int_0^1 g\left((c'+u)e^{it_1} - c' - z_1, \left(b^m + \frac{t_1}{\alpha}\right)^{\frac{1}{m}} \right) \cdot F\left((c'+u)e^{it_1} - c' \right) dv_1 dw_1 \right.$$
$$\left. + e^{-(\lambda+i)t^*} \int_0^1 \int_0^1 g\left(\left(b^m + \frac{t_2}{\alpha}\right)^{\frac{1}{m}} - z_2, \left(b^m + \frac{t_2}{\alpha}\right)^{\frac{1}{m}} \right) \cdot F\left(\left(b^m + \frac{t_2}{\alpha}\right)^{\frac{1}{m}} \right) dv_2 dw_2 \right]$$

with

$$t_1 = -\frac{\log\left(1 - w_1\left(1 - e^{-(\lambda+i)t^*}\right)\right)}{\lambda+i} \qquad z_1 = F^{-1}\left(v_1 \cdot F\left((c'+u)e^{it} - c'\right)\right) \tag{17}$$

$$t_2 = t^* - \frac{\log(1-w_2)}{(\lambda+i)} \qquad z_2 = F^{-1}\left(v_2 \cdot F\left(\left(b^m + \frac{t_2}{\alpha}\right)^{\frac{1}{m}}\right)\right). \tag{18}$$

The Monte Carlo-estimator of $W(u,b)$ for given values of u and b is

$$W(u,b) \approx \frac{1}{N} \sum_{n=1}^{N} g_n^{(k)}(u,b)\ , \tag{19}$$

where the $g_n^{(k)}(u,b)$ are calculated recursively for each n by

$$g_n^{(0)}(u,b) = h(u,b)$$

and

$$g_n^{(i)}(u,b) = h(u,b) + \frac{\lambda}{\lambda+i} \cdot$$
$$\cdot \Bigg\{ F\left((c'+u)e^{it_{1,n}^i} - c'\right)\left(1 - e^{-(\lambda+i)t^*}\right) g_n^{(i-1)}\left((c'+u)e^{it_{1,n}^i} - c' - z_{1,n}^i, \left(b^m + \frac{t_{1,n}^i}{\alpha}\right)^{\frac{1}{m}}\right) +$$
$$+ F\left(\left(b^m + \frac{t_{2,n}^i}{\alpha}\right)^{\frac{1}{m}}\right) e^{-(\lambda+i)t^*} g_n^{(i-1)}\left(\left(b^m + \frac{t_{2,n}^i}{\alpha}\right)^{\frac{1}{m}} - z_{2,n}^i, \left(b^m + \frac{t_{2,n}^i}{\alpha}\right)^{\frac{1}{m}}\right) \Bigg\}.$$

Here $t_{j,n}^i$ and $z_{j,n}^i$ $(j = 1, 2)$ are determined according to (17) and (18) for (quasi-)random deviates v_j, w_j of the uniform distribution in the unit interval $(1 \leq i \leq k)$.

Since in every recursion step the function g is called twice, the number of evaluations of g doubles in every recursion step. Thus, in order to keep the computations tractable, in what we will call the double-recursive algorithm in the sequel, the double recursion is only used for the first three recursive steps and for the remaining recursion steps the recursive algorithm described in Section 3.2 is applied.

3.2 Recursive Algorithm

Instead of calculating the first two integrals occurring in operator (11) separately, one can combine them to one integral. A suitable change of variables then leads to

$$Ag(u,b) = h(u,b) +$$
$$\int_0^1 \int_0^1 \frac{\lambda}{\lambda+i} F\left(z_{max}(u,b,t)\right) g\left(z_{max}(u,b,t) - z, \left(b^m + \frac{t}{\alpha}\right)^{\frac{1}{m}}\right) dvdw \quad (20)$$

where t and z are given by

$$\begin{aligned} t &= -\frac{\log(1-w)}{(\lambda+i)} \\ z &= -F^{-1}\left(v \cdot F(z_{max}(u,b,t))\right) \end{aligned} \quad (21)$$

and $z_{max}(u,b,t)$ is determined by (15). The integral operator (20) is now applied k times onto $g^{(0)}$, and the resulting multidimensional integral $g^{(k)}(u,b)$ is again approximated by

$$g^{(k)}(u,b) \approx \frac{1}{N} \sum_{n=1}^{N} g_n^{(k)}(u,b), \quad (22)$$

where each $g_n^{(k)}(u,b)$ $(n = 1,\ldots,N)$ is based on a pseudo-random (or quasi-random, resp.) point $\mathbf{x}_n \in [0,1]^{2k}$ and calculated by the recursion

$$g_k^{(0)}(u,b) = h(u,b),$$

$$g_n^{(i)}(u,b) = \frac{\lambda}{\lambda+i} F\left(z_{max}(u,b,t_n^i)\right) g_n^{(i-1)}\left(z_{max}(u,b,t_n^i) - z_n^i, \left(b^m + \frac{t_n^i}{\alpha}\right)^{\frac{1}{m}}\right) + h(u,b),$$

with $1 \le i \le k$. t_n^i and z_n^i are given by (21) with v and w being the value of the $(2i)$-th and $(2i+1)$-th, component of $\mathbf{x}_n$, respectively. Note that for this algorithm, the number of integration points needed for a given recursion depth is one eighth of the corresponding number required for the double-recursive case.

3.3 Iterative Algorithm

Another solution technique based on the integral operator (20) is to discretize the domain of u and b by a grid (u_j, b_k), $0 \le j \le j_{max}$, $0 \le k \le k_{max}$. After assigning a suitable initial value to each discretization point (u_j, b_k), the operator is applied sequentially to each point (u_j, b_k) of the grid. The resulting approximative solution $\hat{g}_{j,k}^{(i)}$ at point (u_j, b_k) and iteration depth i is calculated from the values of $\hat{g}^{(i-1)}$ at depth $(i-1)$ by a two-dimensional integral, which is evaluated by Monte Carlo and Quasi-Monte Carlo methods. Since $\hat{g}^{(i-1)}$ is only defined for the discretization points (u_j, b_k), the function $g(z_{max}(u,b,t)-z, (b^m + t/\alpha)^{1/m})$ in operator (20) is replaced by an interpolation function $I(\hat{g}^{(i-1)}, z_{max}(u,b,t) - z, (b^m + t/\alpha)^{1/m})$ defined in (24). Thus we have

$$\begin{aligned}
\hat{g}_{j,k}^{(0)} =& h(u_j, b_k) \\
\hat{g}_{j,k}^{(i)} =& h(u_j, b_k) + \frac{\lambda}{\lambda+i} \cdot \\
& \frac{1}{N}\sum_{n=1}^{N} F\left(z_{max}(u_j, b_k, t_n^i)\right) I\left(\hat{g}^{(i-1)}, z_{max}(u_j, b_k, t_n^i) - z_n^i, \left(b_k^m + \frac{t_n^i}{\alpha}\right)^{\frac{1}{m}}\right)
\end{aligned} \tag{23}$$

for $1 \le i \le i_{max}$. The variables (t_n^i, z_n^i) are obtained from the elements of a 2-dimensional sequence according to (21), and the iteration depth i_{max} does not have to be fixed in advance but may be chosen according to the desired accuracy of the approximation.

In our calculations we use a linear interpolation function for approximating the value of $g^{(i)}$ at point (u,b) with $u_j \le u \le u_{j+1}$ and $b_k \le b \le b_{k+1}$:

$$\begin{aligned}
I(\hat{g}^{(i)}, u, b) = & \left(1 - \frac{u-u_j}{u_{j+1}-u_j}\right)\left(1 - \frac{b-b_k}{b_{k+1}-b_k}\right)\hat{g}_{j,k}^{(i)} + \frac{u-u_j}{u_{j+1}-u_j}\frac{b-b_k}{b_{k+1}-b_k}\hat{g}_{j+1,k+1}^{(i)} + \\
& \left(1 - \frac{u-u_j}{u_{j+1}-u_j}\right)\frac{b-b_k}{b_{k+1}-b_k}\hat{g}_{j,k+1}^{(i)} + \frac{u-u_j}{u_{j+1}-u_j}\left(1 - \frac{b-b_k}{b_{k+1}-b_k}\right)\hat{g}_{j+1,k}^{(i)} .
\end{aligned} \tag{24}$$

If $u_{j+1} > b_k$ (i.e. the left upper corner of the surrounding rectangle lies above $u = b$ and thus outside the valid domain of g), then $g^{(i)}_{j+1,k}$ needs to be replaced by

$$g^{(i)}_{j,k} + g^{(i)}_{j+1,k+1} - g^{(i)}_{j,k+1}$$

in (24) meaning that the plane defined by the remaining three corners is then used for the linear interpolation. If (u, b) lies outside the area that is covered by the grid, the nearest rectangle $((u_j, b_k), (u_{j+1}, b_{k+1}))$ covered by the grid is used for extrapolation by (24).

3.4 Simulation

Another way to obtain numerical solutions is stochastic simulation of the surplus process. For that purpose we sample N paths of the risk reserve process in the following way: Starting with $t_0 := 0$, $b_0 := b$ and $x_0 := u$, where u is the initial reserve of the insurance portfolio, we successively generate exponentially distributed random variables $\tilde{t}_j$ with parameter λ for the time until the next claim occurs and set $t_{j+1} := t_j + \tilde{t}_j$ $(j \in \mathbb{N})$. The claim amount z_j is then sampled from the corresponding claim size distribution by the inversion method, and the reserve after the claim is $x_{j+1} := \min\{(c' + x_j)e^{i\tilde{t}_j} - c', (b_j^m + \tilde{t}_j/\alpha)^{1/m}\} - z_j$. Due to the structure of the dividend barrier, we can reset the origin to t_{j+1} in every step, if we also set $b_{j+1} = \left(b_j^m + \frac{\tilde{t}_j}{\alpha}\right)^{1/m}$. We then have to discount the dividend payments between the j-th and $(j+1)$-th claims by the factor e^{-it_j}.

A simulation estimate for the survival probability $\phi(u, b)$ can now be obtained by

$$\phi(u, b) \approx \frac{m}{N},$$

where m is the number of paths for which ruin does not occur (i.e. $x_j > 0 \ \forall \ j$). We consider a path as having survived, if for some j the condition $x_j > x_{max}$ is fulfilled, where x_{max} is a sufficiently large threshold. This can be viewed as an absorbing horizontal barrier at x_{max}, and so the process stops with probability 1. Using this stopping criterion, we overestimate the actual probability of survival $\phi(u, b)$; for sufficiently large x_{max}, however, this effect is negligible.

For the simulation of the expected value of the dividend payments, we proceed as described above and whenever the process reaches the dividend barrier, i.e. $(c' + x_j)e^{i\tilde{t}_j} - c' > (b_j^m + \tilde{t}_j/\alpha)^{\frac{1}{m}}$, we need to calculate the amount of dividends that are paid until the next claim j occurs:

$$v_j := v_{j-1} + e^{-it_j} \int_{t^*}^{\tilde{t}_j} e^{-is} \left((c + ix_j)e^{is} - \frac{1}{m\alpha \left(b_j^m + \frac{s}{\alpha}\right)^{1-\frac{1}{m}}} \right) ds, \qquad j \geq 1$$

and $v_0 = 0$, where t^* is the positive solution of $(c' + x_j)e^{i\,t} - c' = \left(b_j^m + \frac{t}{\alpha}\right)^{1/m}$, i.e. the time when the process reaches the dividend barrier. The process is stopped, if ruin occurs (i.e. $x_j < 0$ for some j) or at some sufficiently large time t_{max}, after which the expected value of discounted dividends becomes negligible due to the discount factor e^{-it}. Let $v(k)$ now be the final value of v_j for path k. The expected value of the dividends is then approximated by

$$W(u,b) \approx \frac{1}{N}\sum_{k=1}^{N} v(k)\ .$$

3.5 Quasi-Monte Carlo Approach

All the numerical solution techniques described above lead to the numerical evaluation of integrals, which in the classical Monte Carlo algorithm is done by using pseudo-random numbers. However, the use of deterministic uniformly distributed instead of pseudo-random point sequences has proven to be an efficient extension of the classical Monte Carlo method. A well-known measure for the uniformness of the distribution of a sequence $\{\mathbf{x}_n\}_{1\le n\le N}$ in $U^s := [0,1)^s$ is the star-discrepancy

$$D_N^*(\mathbf{x}_n) = \sup_{I\in J_0^s}\left|\frac{A(\mathbf{x}_n;I)}{N} - \lambda_s(I)\right|\ ,$$

where J_0^s is the set of all intervals of the form $[0,\mathbf{y}) = [0,y_1)\times[0,y_2)\times\ldots\times[0,y_s)$ with $0 \le y_i < 1$, $i = 1,\ldots,s$ and $A(\mathbf{x}_n;I)$ is the number of points of the sequence $\{\mathbf{x}_n\}_{1\le n\le N}$ that lie in I. $\lambda_s(I)$ denotes the s-dimensional Lebesgue-measure of I.

The notion of discrepancy is particularly useful for obtaining an upper bound for the error of Quasi-Monte Carlo integration, since by the Koksma-Hlawka inequality, we have

$$\left|\frac{1}{N}\sum_{n=1}^{N} f(x_n) - \int_{[0,1)^s} f(u)du\right| \le V([0,1)^s, f)D_N^*\left(x_1,\ldots,x_N\right)\ . \tag{25}$$

for any set of points $\{x_1,\ldots,x_N\} \subset [0,1)^s$ and for any function $f : [0,1)^s \to \mathbb{R}$ of bounded variation $V([0,1)^s, f)$ in the sense of Hardy and Krause (see e.g. [12]).
This error bound is deterministic (in contrast to error bounds obtainable for classical Monte Carlo). Especially for s not too large, certain Quasi-Monte Carlo sequences have turned out to be superior to pseudo-Monte Carlo sequences in many applications. This is in particular the case for so-called *low discrepancy sequences*, i.e. sequences for which

$$D_N^*\left(x_1,\ldots,x_N\right) \le C_s\frac{(\log N)^s}{N}, \tag{26}$$

with an explicitly computable constant C_s, holds. Bounds for C_s are usually pessismistic and often the actual error made by Quasi-Monte Carlo integration is much lower than

the bound implied by C_s (see e.g. [9]). Some low discrepancy sequences will be given in the sequel:

- The Halton sequence [18] is defined as a sequence of vectors in U^s based on the digit representation of n in base p_i

$$\xi_n = (b_{p_1}(n), b_{p_2}(n), \ldots, b_{p_s}(n)), \tag{27}$$

where p_i is the ith prime number and $b_p(n)$ is the digit reversal function for base p given by

$$b_p(n) = \sum_{k=0}^{\infty} n_k p^{-k-1}, \qquad n = \sum_{k=0}^{\infty} n_k p^k,$$

where the n_k are integers. One could also use pairwise coprime base numbers, but the error estimate turns out to be the best possible for prime bases p_n.

Better error bounds can be obtained for low-discrepancy sequences based on so-called (t, m, s)-nets or nets for short. These nets are based on the b-adic representation of vectors in U^s. Instead of optimizing the discrepancy itself, one considers the discrepancy with respect to elementary intervals J in base b only, i.e. $J = \prod_{i=1}^{s} [a_i b^{-d_i}, (a_i + 1)b^{-d_i})$ with integers $d_i \geq 0$ and integers $0 \leq a_i < b^{d_i}$ for $1 \leq i \leq s$, and tries to construct point sequences in U^s such that the discrepancy with respect to these intervals J is optimal for subsequences of length $N = b^m$.
Let $\#(J, N)$ denote the number of points of a sequence $\{\mathbf{x}_n\}_{1 \leq n \leq N}$ that lie in J. A point set $\mathcal{P}$ with $\mathrm{card}(\mathcal{P}) = b^m$ is now called a (t, m, s)-net, if

$$\#(J, b^m) = b^t$$

for every elementary interval J with $\lambda_s(J) = b^{t-m}$. The parameter t is a quality parameter. For $t = 0$ we have the minimal discrepancy of the point set $\mathcal{P}$ with respect to the family of elementary intervals.

Definition: Let $t \geq 0$ be an integer. A sequence $\xi_1, \xi_2, \ldots$ of points in U^s is called a (t, s)-sequence in base b, if for all integers $k \geq 0$ and $m > t$, the point set consisting of the ξ_n with $kb^m < n \leq (k+1)b^m$ is a (t, m, s)-net in base b.

Examples of (t, m, s)-nets are:

- The Sobol Sequence is a (t, s)-sequence in base 2 with values t that depend on s. For a construction of this sequence we refer to [25].
- Faure sequences are low-discrepancy sequences for which C_s tends to zero for $s \to \infty$ (see e.g. [13]).

- The Niederreiter sequences (cf. [20]) yield (t, s)-sequences in arbitrary base; among them there are $(0, s)$-sequences in prime power bases $b \geq s$. In particular, for Niederreiter sequences the constant C_s in (26) tends to zero for $s \to \infty$.

4 Numerical Results for the parabolic case

In this section we present numerical results for a parabolic dividend barrier of the form $b_t = \sqrt{b^2 + t/\alpha}$ and various claim amount distributions. Note that in this case, t^* is the solution of the equation

$$(c' + u)e^{it^*} - c' = \left(b^2 + \frac{t^*}{\alpha}\right)^{1/2} ,$$

which needs to be calculated numerically, and the inhomogeneous term $h(u, b)$ in (11) can be calculated to

$$h(u, b) = e^{-\lambda t^*} \left(\frac{c + iu}{\lambda} - \frac{e^{-it^*} e^{z^2}}{2} \sqrt{\frac{\pi}{(\lambda + i)\alpha}}\, erfc(z) \right)$$

with $z = \sqrt{(\lambda + i)(\alpha b^2 + t^*)}$.

4.1 General Remarks

Table 1 gives the choice of the parameter values and the densities of the claim size distributions used in our calculations. The corresponding distribution parameters are chosen such that the mean and variance of the distributions coincide and are equal to 1 and 0.5, respectively. Three of the four distributions are heavy-tailed.

The MC and QMC estimates are obtained using $N = 66\,000$ paths for the recursive case and for the simulation and $N = 33\,000$ for the double-recursive and iterative calculations. Since exact values are not available, we estimated them by a MC-simulation over 10 million paths for every choice of u and b.

For the recursive and double recursive calculations we use a recursion depth of $k = 66$, which leads to a 132-dimensional sequence needed for the MC- and QMC-calculations, while for the simulation it turned out to be sufficient to take a 400-dimensional sequence so that 200 consecutive claims and interoccurrence times of a risk reserve sample path can be simulated from one element of the sequence and correlations among the claim sizes and claim occurrence times are avoided.

	Parameter	Values
b	height of dividend barrier at time $t = 0$	0..[0.1]..1
u	initial capital	0..[0.1]..b
c	premium density	1.5
λ	intensity of claim number process	1
i	constant interest force	0.1
α	dividend barrier parameter	0.5
t_{max}	stopping criterion for simulations	100
b_{max}	absorbing upper barrier in Model B	4

Claim size distributions	density
Gamma $(2, 2)$	$f(x) = 4x\, e^{-2x}$
Lognormal $(-0.203, 0.637)$	$f(x) = \frac{1}{\sqrt{2\pi}\cdot 0.637\cdot x}\, e^{-\frac{(\log x + 0.203)^2}{2(0.637)^2}}$
Pareto $(2.732, 0.634)$	$f(x) = 0.786 \frac{1}{x^{3.732}}$
Weibull $(1.44, 1.10)$	$f(x) = 1.31 \left(\frac{x}{1.1}\right)^{0.44} e^{-\left(\frac{x}{1.1}\right)^{1.44}}$

Table 1: Parameter values and claim size distributions

For the iterative calculations we use a depth of $i_{max} = 66$ and enlarge the grid to $b = 7$ so that the extrapolation from the array in $0 \leq u \leq b \leq 1$ is sufficiently accurate.

All our QMC-calculations are actually hybrid Monte Carlo estimates, i.e. the initial 50 dimensions are generated by a 50-dimensional QMC sequence and the remaining dimensions are generated by a pseudo-random number generator. The use of hybrid Monte Carlo sequences has proven to be a successful modification of the QMC-technique, since for low discrepancy sequences typically the number of points needed to obtain a satisfying degree of uniformness dramatically increases with the number of dimensions. Moreover, due to the nature of our risk reserve process, the initial dimensions of the sequence have a higher impact on the solution than higher dimensions.
Throughout this paper, we use `ran2` as our pseudo-random number generator as described in [22], which basically is an improved version of a Minimal Standard generator based on a multiplicative congruential algorithm.

The different methods and sequences used are compared via the mean square error (MSE)

$$S = \sqrt{\frac{1}{|P|} \sum_{(u,b)\in P} \Big(g(u,b) - \tilde{g}(u,b)\Big)^2},$$

where $g(u,b)$ and $\tilde{g}(u,b)$ denote the exact and the approximated value, respectively, and the set P is a grid in the triangular region $(b = 0..[0.1]..1, u = 0..[0.1]..b)$. In addition, for each method we give the maximal deviation of the approximated value from the corresponding exact value $\|\Delta\|_\infty = \max_{(u,b)\in P}\Big(g(u,b) - \tilde{g}(u,b)\Big)$.

The simulations showed that the implementation of Faure and Niederreiter $(0,s)$-sequences cannot compete with the performance of other low-discrepancy sequences for the integrands of our problems. Therefore the simulation results of these two sequences have not been included in the following considerations.

4.2 Error analysis

4.2.1 Survival probability

In Model A the survival probability can only be calculated using the simulation approach. Figure 2 shows the errors for the Weibull distribution and Table 2 gives the mean-square and the maximal error of the simulation results for each of the sequences and claim size distributions used ($N = 66\,000$).

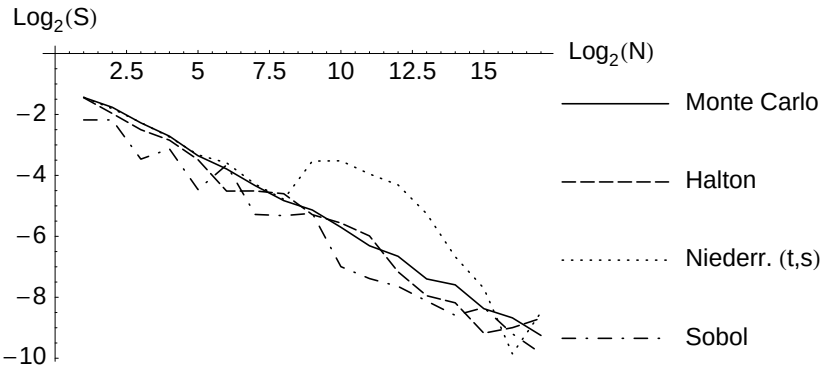

Figure 2: MSE of the simulation of $\phi(u,b)$ as a function of N (Model A, Weibull distribution)

Here, only the Sobol sequence leads to an improvement compared to the Monte Carlo simulation.

In Model B, the integral operator (14) can be used to calculate the survival probability,

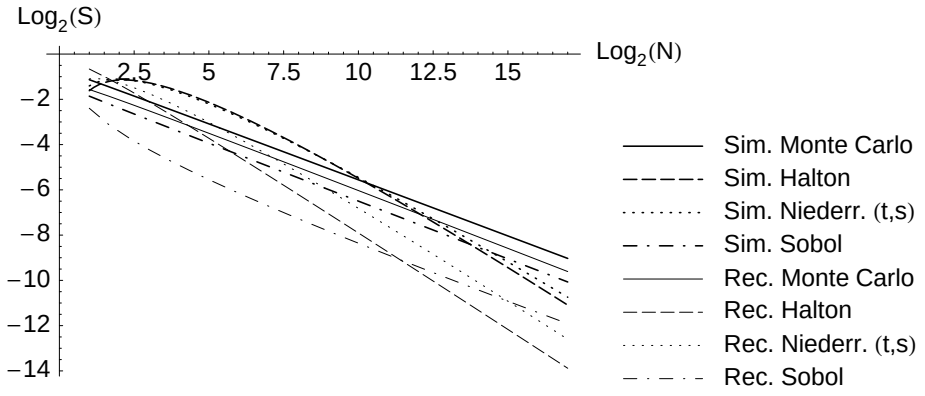

Figure 3: MSE of $\phi(u, b)$ estimates as a function of N (Pareto distribution, Model B), fitted

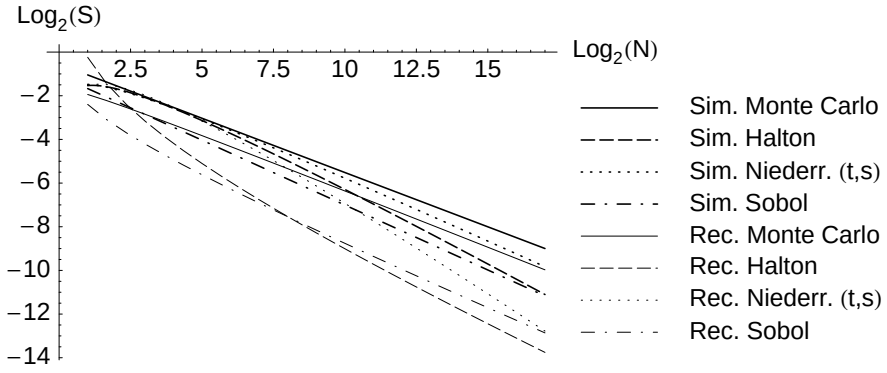

Figure 4: Fitted MSE of $\phi(u, b)$ estimates (Gamma distribution, Model B)

		Monte Carlo	Halton	Niederr. (t,s)	Sobol
Gamma	S	0.001744	0.002247	0.002585	0.001111
	$\|\Delta\|_\infty$	0.004195	0.004773	0.004595	0.002393
Lognormal	S	0.001648	0.001678	0.001813	0.001437
	$\|\Delta\|_\infty$	0.003738	0.004164	0.003402	0.002687
Pareto	S	0.001888	0.002119	0.002043	0.002695
	$\|\Delta\|_\infty$	0.004477	0.004285	0.005239	0.00431
Weibull	S	0.001632	0.002423	0.002656	0.001141
	$\|\Delta\|_\infty$	0.00463	0.004685	0.004179	0.002338

Table 2: Simulation errors for the survival probability in Model A

		Monte Carlo	Halton	Niederr. (t,s)	Sobol
Gamma					
Simulation	S	0.00186705	0.000698195	0.00180109	0.000303748
	$\|\Delta\|_\infty$	0.004275	0.001265	0.003022	0.000612
Recursive	S	0.00115668	0.000148828	0.000216361	0.000157103
	$\|\Delta\|_\infty$	0.003236	0.000331	0.000486	0.00036
Iterative	S	0.010934	0.0107691	0.0108299	0.0108279
	$\|\Delta\|_\infty$	0.015	0.013732	0.013807	0.013803
Lognormal					
Simulation	S	0.0018042	0.000351439	0.00195453	0.000282303
	$\|\Delta\|_\infty$	0.004136	0.001045	0.003431	0.000923
Recursive	S	0.00119801	0.000146449	0.000221486	0.000187532
	$\|\Delta\|_\infty$	0.0033	0.000332	0.000523	0.000424
Iterative	S	0.0115233	0.0113429	0.01141	0.011408
	$\|\Delta\|_\infty$	0.015954	0.014688	0.014772	0.014767
Pareto					
Simulation	S	0.00187995	0.000494491	0.00159844	0.000652944
	$\|\Delta\|_\infty$	0.004005	0.001343	0.003035	0.001666
Recursive	S	0.00144045	0.000177989	0.000210099	0.000208204
	$\|\Delta\|_\infty$	0.003893	0.000513	0.000539	0.00044
Iterative	S	0.0131512	0.0129077	0.0129771	0.012975
	$\|\Delta\|_\infty$	0.018795	0.01741	0.017498	0.017498
Weibull					
Simulation	S	0.0017325	0.000530047	0.00132312	0.000342577
	$\|\Delta\|_\infty$	0.004521	0.001225	0.002562	0.000812
Recursive	S	0.00114726	0.000155255	0.000215812	0.000147719
	$\|\Delta\|_\infty$	0.003259	0.000377	0.00047	0.00036
Iterative	S	0.0106633	0.0105005	0.0105598	0.0105578
	$\|\Delta\|_\infty$	0.014519	0.013309	0.013382	0.013378

Table 3: Simulation errors for the survival probability in Model B

and the errors of the different methods are given in Table 3.

To quantify the effect of using a low discrepancy sequence, we perform a regression analysis by fitting

$$\log_2(S) = a_0 + a_1 \log_2(N) + a_2 \log_2(\log_2(N)) + \epsilon$$

to the data using a least square fit. Note that Koksma-Hlawka's inequality (25) could be interpreted as implying $a_1 = -1$ and $a_2 = s$, where s is the dimension of the sequence used. However, since we use a hybrid sequence and since the effective dimension may differ from the theoretical dimension, the values of a_1 and a_2 deviate from the ones above. Figures 3 and 4 show these regression fits for the Pareto and Gamma distributions, the Weibull and Lognormal distributions show a similar behaviour. In the sequel, all figures will be given in terms of their regression fits.

4.2.2 Expected value of the dividend payments

The simulation results for the expected value of the dividends in Model A show a clear advantage of QMC methods over MC integration. As an illustration, Figure 5 depicts the MSE of the simulation results as a function of N for the Weibull distribution.

While for small N, the Sobol sequence outperforms the other sequences by a factor of about 4 in terms of the MSE, for large N the Halton sequence used in the recursive algorithm is to be preferred. To quantify this effect, we introduce the efficiency gain

$$gain_i = \frac{N^*_{\mathrm{MC}}(S)}{N^*_i(S)}$$

where $N^*_{\mathrm{MC}}(S)$ is the number of paths needed in the Monte Carlo simulation to reach a given error of S, and $N^*_i(S)$ is the corresponding N using an alternative method. Figure 6 shows that except for the $(0, s)$-nets (which are not plotted) all methods are an improvement in efficiency compared to Monte Carlo simulation and the gain increases at smaller errors.

The above comparisons are performed with respect to N, the number of summands in the MC and QMC approximations. However, it might be preferable to compare the accuracy of the various numerical solution techniques with respect to calculation time, see Table 4 and Figure 7. It turns out that the performance of the double recursive algorithm is still competitive when measured with respect to calculation time; however, the recursive method using Sobol's sequence seems preferable. One also has to notice that the Niederreiter sequence in base 2 gives results worse than the Monte Carlo methods, which is due to the fact that in Model A, all 50 QMC dimensions of the elements are relevant. However, the quality of the different sequences also depends on the claim

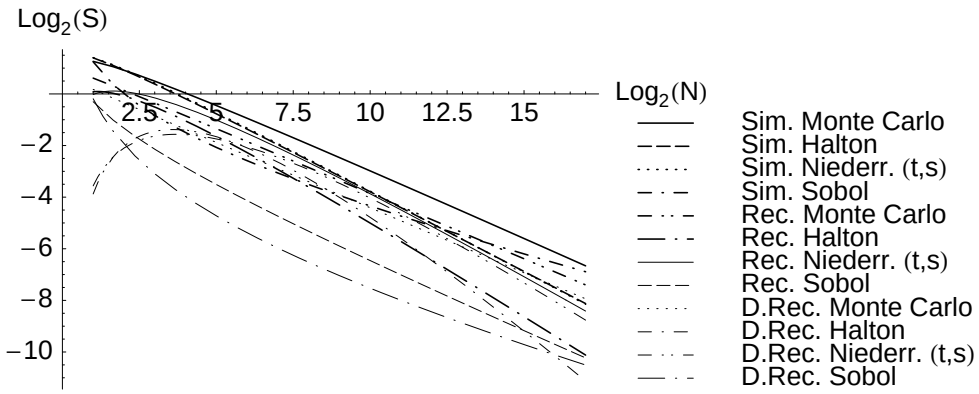

Figure 5: MSE of expected dividend payments (Weibull distribution, Model A)

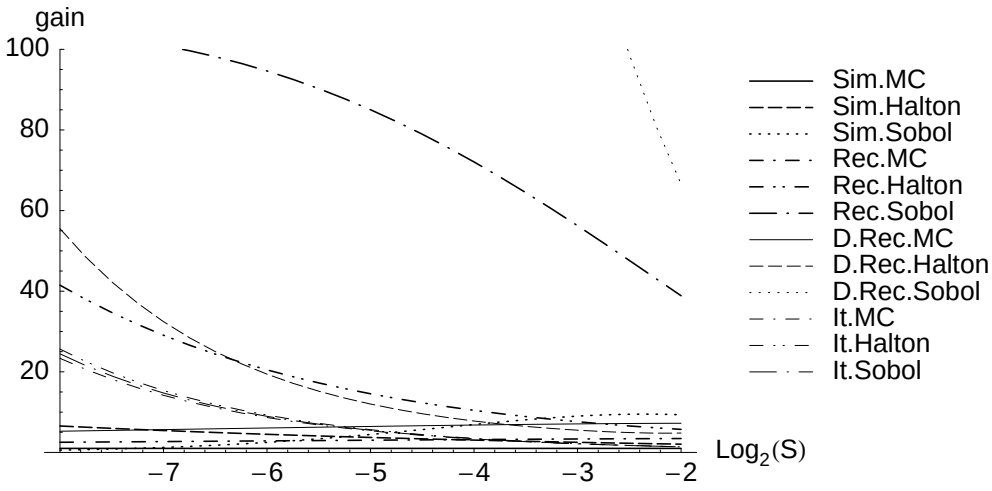

Figure 6: Efficiency gain for calculation of expected dividends (Model A, Weibull distribution)

distribution used, as a comparison with Figure 8 shows. Moreover, it is clearly visible that although the simulation is the fastest method using N elements, it is actually the worst when the error is considered.

	Simulation	Iterative	Recursive	Double Rec.
Monte Carlo	209.551	413.685	746.824	3062.61
Halton	186.033	407.416	802.648	3162.44
Niederr. (t,s)	250.527	388.903	732.736	3036.35
Sobol	186.813	174.247	947.162	2811.14
Faure	393.982	174.3	732.161	3028.67
(0,s) net	179.47	389.017	732.048	3028.34

Table 4: Calculation times in seconds (expected dividends, Lognormal distribution, Model A)

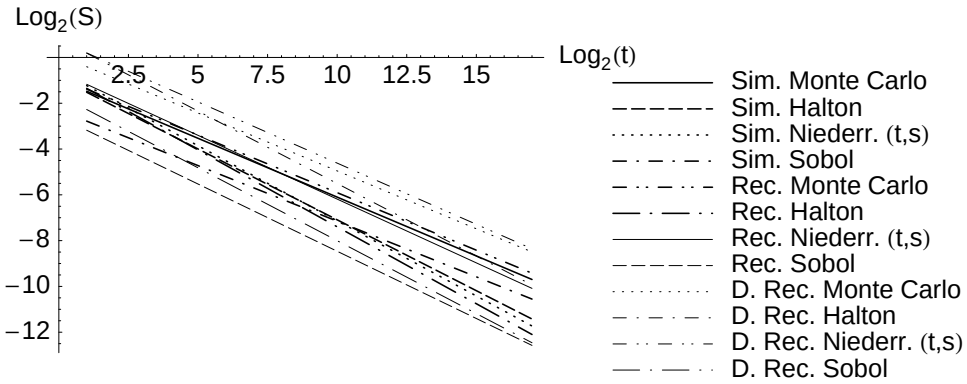

Figure 7: MSE of the expected dividend payments as a function of calculation time (Lognormal distribution, Model A)

Figure 8 furthermore shows an attempt to compare the results of the iterative method with the other methods. Here some care is needed, since the recursion depth k of the recursive algorithms is fixed in advance (and thus also the error caused by choosing k) and the number N of sequence elements is increased with time. On the other hand, for the iterative method N is fixed in advance and the iteration depth is increased with time.

The calculations show that for all iterative methods and the above choice of initial values, it takes 40 to 50 iterations until the approximations are sufficiently close to the exact values. Thus one might try to improve the efficiency of the algorithm by first simulating the process (with a small number N_s of simulation paths) and then use these simulation estimates as initial values for the iterative procedure. Naturally, this choice of initial values for the grid has a much lower initial error than using $h(u_j, b_k)$, but is

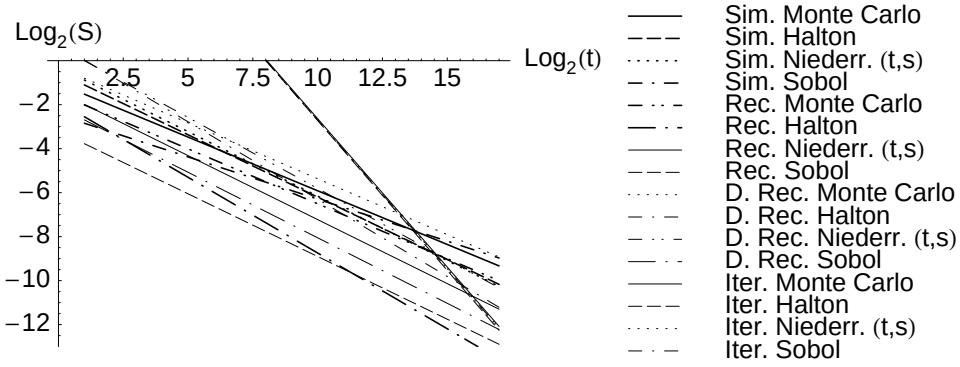

Figure 8: Calculation times in seconds (expected dividend payments, Pareto distribution, Model A)

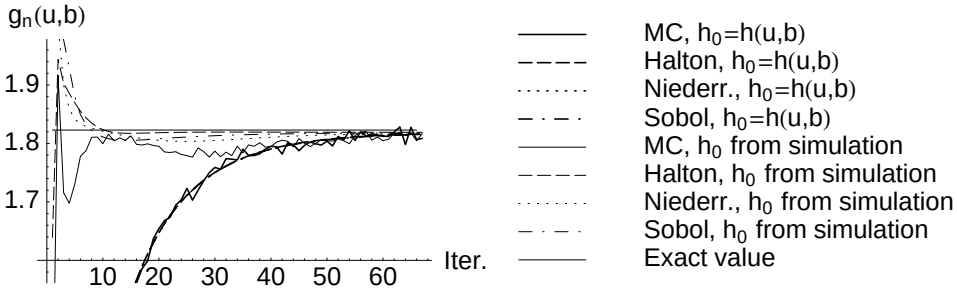

Figure 9: Convergence of the dividend payments estimate for $(u, b) = (0, 1)$ (iterative method using $h(u, b)$ and 10 simulation paths, resp., as initial values for the grid, Lognormal Distribution, Model A)

much less smooth than h which lowers the convergence rate of the algorithm. However, Figure 9 shows that even for $N_s = 10$, this approach substantially improves the plain iterative method.

In contrast to Model A, in Model B the effective dimension of the simulation as well as the dimension of the iterated integral operator becomes very small. It turns out that for the Weibull, Gamma and Lognormal distribution on average only about 8 claims or iterations of the operator are needed until b becomes large enough so that practically no dividends will be paid out any more, and for the Pareto distribution only 3 to 6 claims are needed. So while Model A is a high-dimensional problem (with 50 QMC dimensions in our case), Model B is low-dimensional with an effective dimension of less than 20 (every claim or recursive step needs two dimensions), and one can expect the usual good properties for low-discrepancy sequences in low-dimensional environments. Figure 10 shows the MSE as a function of N for the Gamma distribution. The behavior is similar to Model A, except that now the (t, s) nets exhibit a good convergence which is even better than Halton's sequence (other distributions also show a similar behaviour). Here again, Sobol's sequence is by far the best for a low number N of points, but loses quality for larger N (cf. Figure 11). Figure 12 depicts the MSE as a function of calculation time.

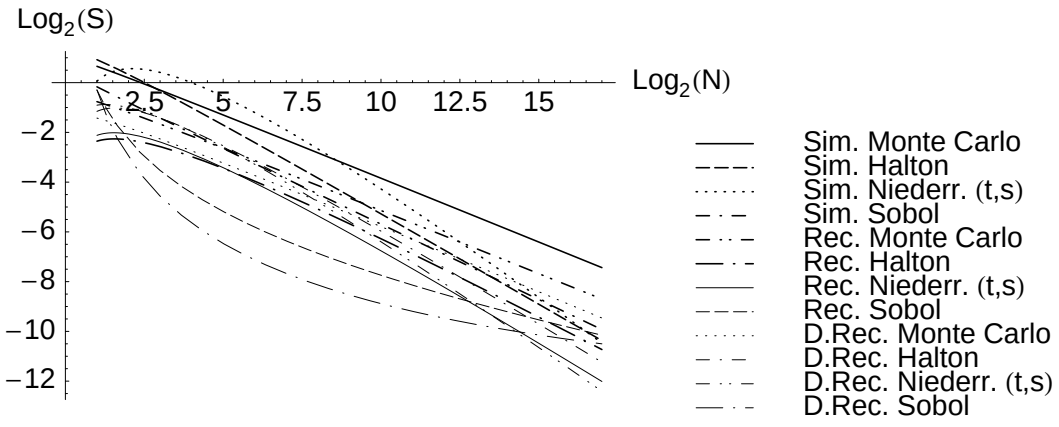

Figure 10: MSE of expected dividend payments (Gamma distribution, Model B)

As pointed out by Bratley, Fox and Niederreiter [7] and numerically investigated by Radovic, Sobol' and Tichy [23], the distribution behavior of the initial elements of (t, s) nets is not satisfying due the so-called leading-zeros phenomenon. Thus, it has been suggested to start the sequence at $n = p^k$ (called the "step"), with k being at least the maximum degree of the polynomials used to generate the sequence and p denoting the base of the construction. As Figure 13 shows, introducing the step indeed

considerably improves the performance of (t, s)-sequences for moderate sizes of N.

The iterative method in Model B is very sensitive to the choice of the mesh-size of the grid, so that one has to select a very small mesh-size to get good results. It turns out that for a mesh-size of 0.5 and 0.2 for values of $b > 1$ up to $b = 4$ (when no dividends will be paid out any more due to the absorbing barrier), the obtained values typically still are about 0.02 and 0.003, respectively, greater than the exact value.

Tables 5 and 6 give a complete list of all the errors of the various methods for all distributions in Model A and B, respectively.

4.3 Model Analysis

In this final section we want to use our simulation results to investigate the sensitivity of the probability of survival and the expected dividend payments to the claim size distribution and to the consideration of interest rates. For that purpose we fix a value of b (the initial height of the dividend barrier) and plot $\phi(u, b)$ and $W(u, b)$ against u. Figures 14 and 15 depict $\phi(u, b)$ for the choice $b = 1$ in Model A and B, respectively. They also include the corresponding plot for $i = 0$. Note that all the distributions are normalized to have equal mean and variance. Since heavy tail distributions exhibit their characteristic behavior for larger values of u, we also give a plot of $\phi(u, b)$ against u for $b = 30$ in Model A (Figure 16).

A double logarithmic plot of the ruin probability (Figure 17) against u (for fixed $b = 30$) displays a similar behaviour of the heavy-tail distributions in our dividend barrier model as it has been obtained by simulation of surplus processes without a barrier (see e.g. Asmussen and Binswanger [6]). Note that the Pareto distribution implies a qualitatively different behavior of $\phi(u, b)$ for large u. Related simulations have shown that for larger values of the variance, this is also the case for Log-normal distributions (cf. Heersink [19]).

Figures 18 and 19 show the dependence of the expected dividend payments on u for fixed values of $b = 1$ and $b = 30$, respectively. Here it turns out that the consideration of gaining interest on the free reserve has a large effect on the values of $W(u, b)$, whereas the choice of the claim size distribution is more or less negligible.

As an illustration Tables 7 to 10 give the exact values of $\phi(u, b)$ and $W(u, b)$ for the Gamma distribution in Model A and B, respectively (a complete list of all the exact and simulated values is available from the authors).

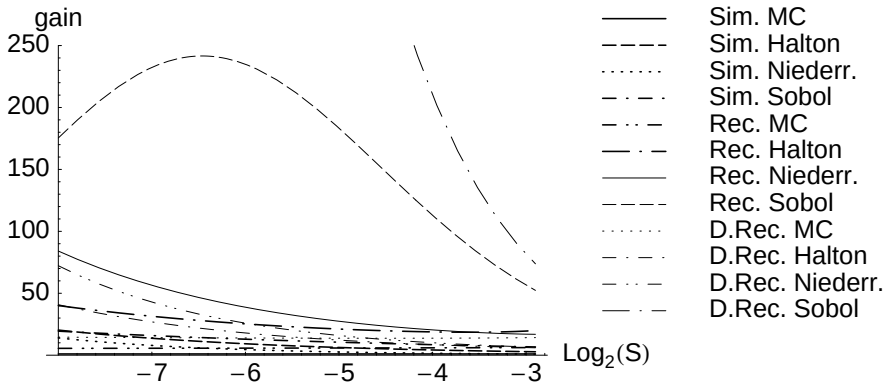

Figure 11: Efficiency gain for calculation of expected dividends (Model B, Gamma distribution)

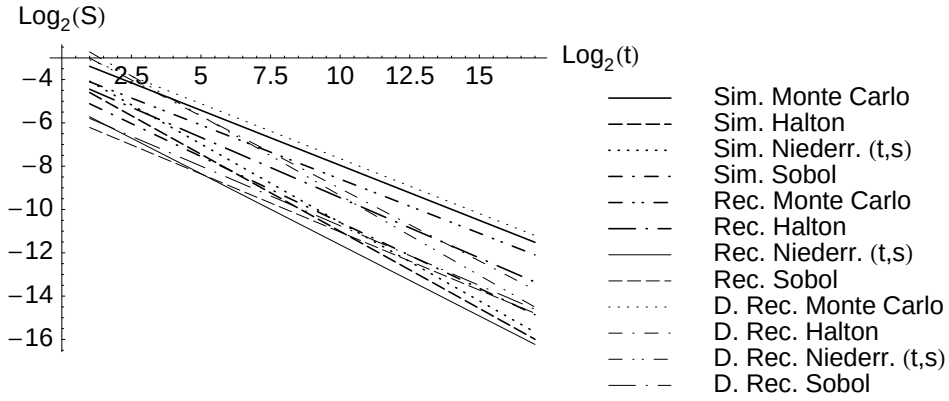

Figure 12: MSE of expected dividend payments (Gamma distribution, Model B) as a function of calculation time

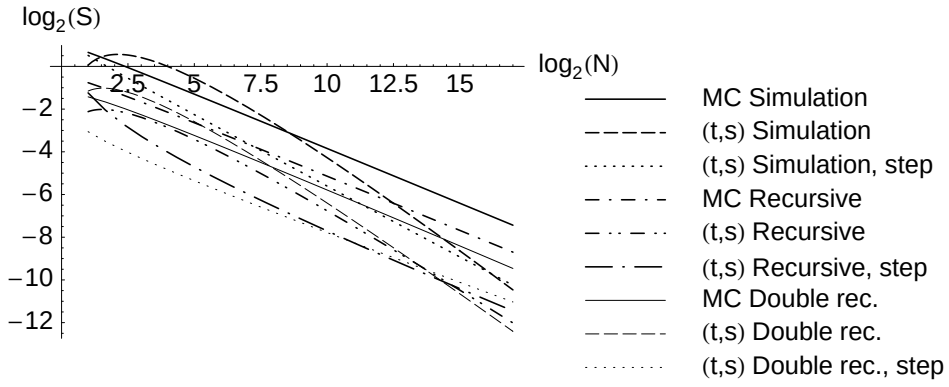

Figure 13: MSE of expected dividends, step=53^3 (Gamma distribution, Model B)

		Monte Carlo	Halton	Niederr. (t,s)	Sobol
Gamma					
Simulation	S	0.0102387	0.00589075	0.00644128	0.0122924
	$\|\Delta\|_\infty$	0.02573	0.01542	0.01382	0.01653
Recursive	S	0.00690747	0.00186699	0.00504432	0.00138267
	$\|\Delta\|_\infty$	0.02303	0.00331	0.00699	0.00274
Double Rec.	S	0.00699453	0.00185775	0.00333911	0.00110242
	$\|\Delta\|_\infty$	0.01626	0.00362	0.00535	0.00249
Iterative	S	0.016958	0.0153584	0.0160474	0.0160834
	$\|\Delta\|_\infty$	0.02798	0.02057	0.02143	0.02146
Lognormal					
Simulation	S	0.0104705	0.00609589	0.00585217	0.0139076
	$\|\Delta\|_\infty$	0.02215	0.01477	0.01377	0.01843
Recursive	S	0.00719265	0.00164129	0.00622522	0.0016576
	$\|\Delta\|_\infty$	0.02355	0.00323	0.00863	0.00296
Double Rec.	S	0.00708872	0.00148873	0.00484965	0.00100742
	$\|\Delta\|_\infty$	0.01592	0.00319	0.00739	0.00248
Iterative	S	0.0170572	0.0154885	0.0162279	0.0162694
	$\|\Delta\|_\infty$	0.02873	0.02154	0.0225	0.02254
Pareto					
Simulation	S	0.0111856	0.0130283	0.0127553	0.0221408
	$\|\Delta\|_\infty$	0.0297	0.0237	0.02513	0.0275
Recursive	S	0.00828872	0.00167252	0.00790734	0.00251632
	$\|\Delta\|_\infty$	0.02591	0.00407	0.0114	0.00455
Double Rec.	S	0.00767502	0.00131978	0.00807013	0.00119566
	$\|\Delta\|_\infty$	0.01775	0.00371	0.0114	0.00322
Iterative	S	0.0216169	0.0206179	0.0213459	0.0214136
	$\|\Delta\|_\infty$	0.03623	0.02909	0.03007	0.03013
Weibull					
Simulation	S	0.00985157	0.005163	0.00685562	0.012519
	$\|\Delta\|_\infty$	0.02465	0.01205	0.01505	0.01741
Recursive	S	0.0068602	0.00201594	0.00457433	0.00133397
	$\|\Delta\|_\infty$	0.02297	0.00354	0.00627	0.00272
Double Rec.	S	0.00699997	0.00211651	0.002768	0.00110075
	$\|\Delta\|_\infty$	0.01634	0.00384	0.00449	0.00236
Iterative	S	0.016865	0.0152578	0.0159104	0.0159438
	$\|\Delta\|_\infty$	0.02783	0.02037	0.02119	0.02122

Table 5: Errors of the various methods for expected dividend payments in Model A

		Monte Carlo	Halton	Niederr. (t,s)	Sobol
Gamma					
Simulation	S	0.00548782	0.00101735	0.000896726	0.00102161
	$\|\Delta\|_\infty$	0.01285	0.00238	0.00201	0.00246
Recursive	S	0.00258046	0.000573281	0.00048327	0.000696459
	$\|\Delta\|_\infty$	0.00652	0.00171	0.00151	0.00201
Double Rec.	S	0.00237654	0.00062463	0.000638122	0.000951905
	$\|\Delta\|_\infty$	0.00559	0.00185	0.00188	0.00239
Iterative	S	0.0176776	0.018468	0.0183926	0.018383
	$\|\Delta\|_\infty$	0.02558	0.02328	0.02317	0.02316
Lognormal					
Simulation	S	0.00496058	0.000959204	0.00115588	0.000858514
	$\|\Delta\|_\infty$	0.01278	0.00206	0.00274	0.00289
Recursive	S	0.00263774	0.000567729	0.000465821	0.000696362
	$\|\Delta\|_\infty$	0.00689	0.00182	0.00161	0.00215
Double Rec.	S	0.00229559	0.000588638	0.000605718	0.000989495
	$\|\Delta\|_\infty$	0.00526	0.00193	0.00197	0.00256
Iterative	S	0.0216594	0.0225257	0.0224476	0.0224349
	$\|\Delta\|_\infty$	0.03055	0.02876	0.02864	0.02864
Pareto					
Simulation	S	0.005052	0.000733847	0.00111069	0.000917839
	$\|\Delta\|_\infty$	0.01517	0.00156	0.00292	0.00219
Recursive	S	0.0028135	0.000453588	0.000424179	0.000635163
	$\|\Delta\|_\infty$	0.00802	0.00166	0.00156	0.00204
Double Rec.	S	0.00197331	0.000496007	0.000579632	0.000935201
	$\|\Delta\|_\infty$	0.003926	0.00178	0.00203	0.00245
Iterative	S	0.0301029	0.0310616	0.031024	0.0310033
	$\|\Delta\|_\infty$	0.04231	0.04179	0.04173	0.04171
Weibull					
Simulation	S	0.00533089	0.000849476	0.000803501	0.000875673
	$\|\Delta\|_\infty$	0.0136	0.00242	0.00216	0.00203
Recursive	S	0.00257658	0.000570681	0.000486129	0.000688766
	$\|\Delta\|_\infty$	0.00652	0.00178	0.00158	0.00207
Double Rec.	S	0.00241979	0.000619308	0.000643352	0.000921779
	$\|\Delta\|_\infty$	0.00572	0.00191	0.00196	0.00243
Iterative	S	0.016305	0.0170657	0.0169917	0.016983
	$\|\Delta\|_\infty$	0.02382	0.02149	0.02138	0.02138

Table 6: Errors of the various methods for expected dividend payments in Model B

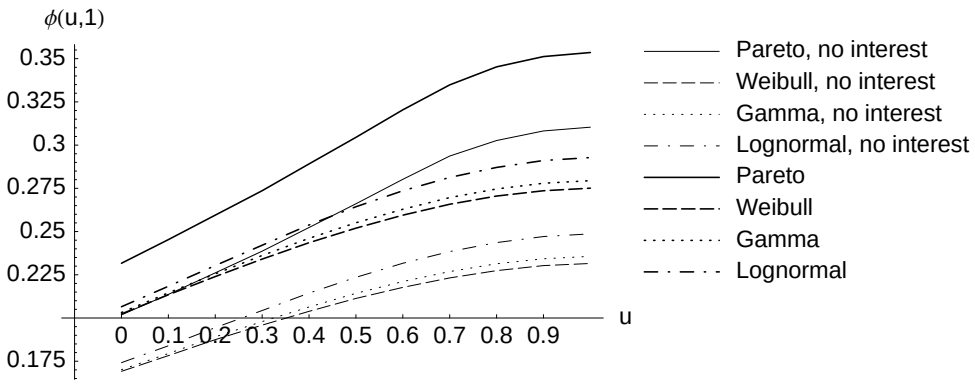

Figure 14: Survival probability $\phi(u, 1)$ in Model A

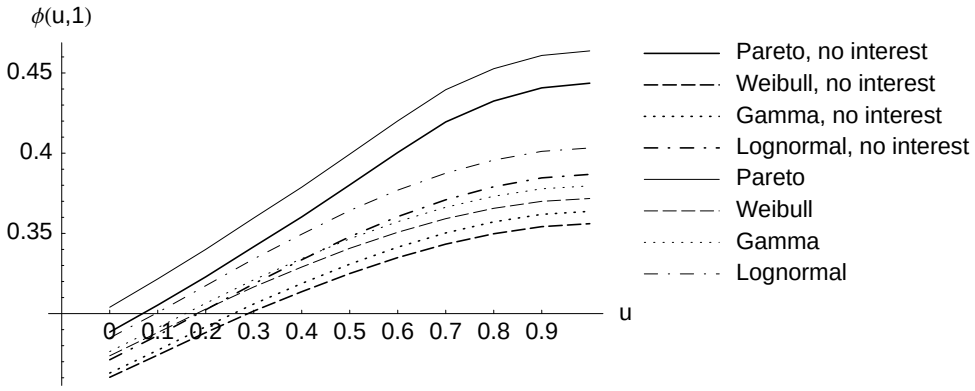

Figure 15: Survival probability $\phi(u, 1)$ in Model B

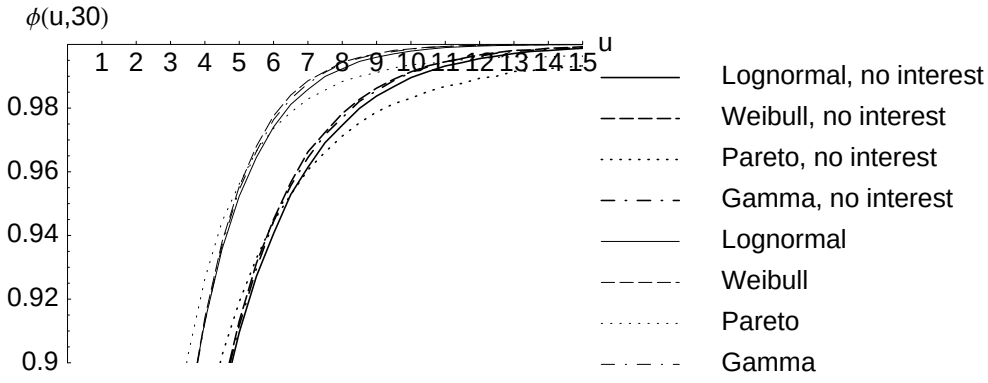

Figure 16: Survival probability $\phi(u, 30)$ in Model A

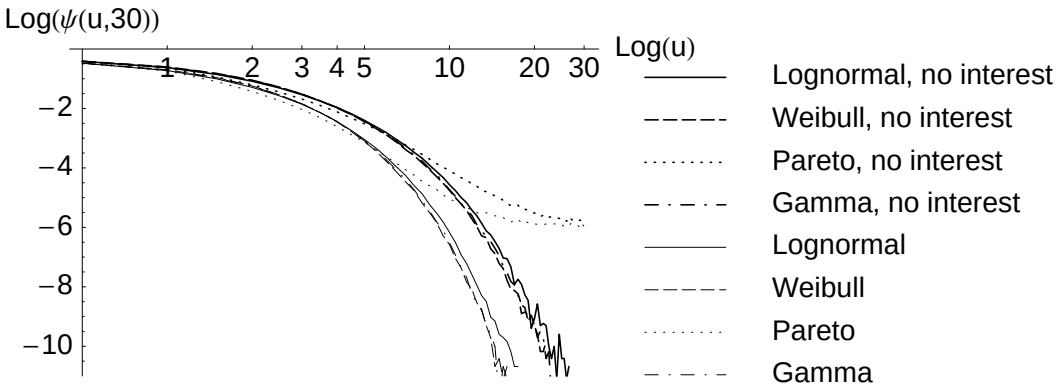

Figure 17: Log-log plot of the ruin probability $\psi(u, 30)$ against u (Model A)

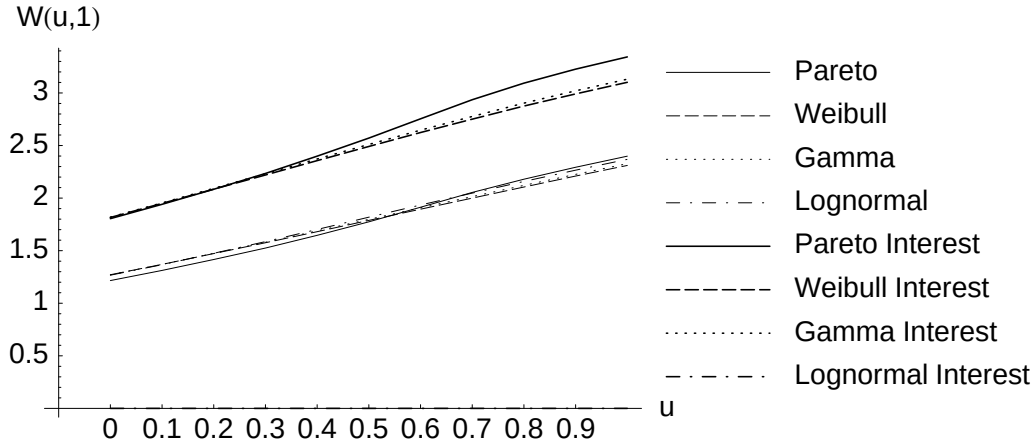

Figure 18: Expected dividend payments $W(u, 1)$ in Model A

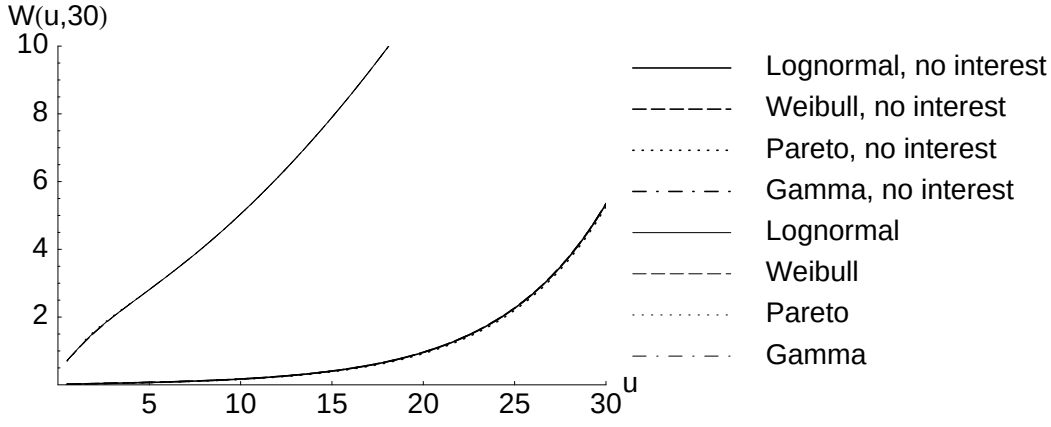

Figure 19: Expected dividend payments $W(u, 30)$ in Model A

$b\backslash x$	0	0.1	0.2	0.3	0.4	0.5	0.6	0.7	0.8	0.9	1.
0	0.18										
0.1	0.18	0.188									
0.2	0.181	0.189	0.197								
0.3	0.182	0.191	0.199	0.206							
0.4	0.184	0.193	0.201	0.209	0.214						
0.5	0.187	0.196	0.204	0.212	0.219	0.223					
0.6	0.189	0.199	0.208	0.217	0.224	0.23	0.233				
0.7	0.193	0.202	0.212	0.221	0.229	0.235	0.241	0.243			
0.8	0.196	0.206	0.216	0.226	0.235	0.242	0.248	0.252	0.254		
0.9	0.2	0.21	0.221	0.231	0.24	0.249	0.256	0.261	0.265	0.266	
1.	0.203	0.215	0.226	0.236	0.246	0.255	0.263	0.27	0.275	0.278	0.279

Table 7: Exact values for the survival probability of the Gamma distribution, Model A

$b\backslash x$	0	0.1	0.2	0.3	0.4	0.5	0.6	0.7	0.8	0.9	1.
0	1.78										
0.1	1.782	1.904									
0.2	1.783	1.906	2.036								
0.3	1.785	1.911	2.04	2.17							
0.4	1.789	1.915	2.048	2.177	2.303						
0.5	1.794	1.922	2.053	2.188	2.315	2.436					
0.6	1.799	1.927	2.062	2.196	2.327	2.456	2.572				
0.7	1.805	1.935	2.069	2.205	2.339	2.468	2.594	2.709			
0.8	1.811	1.942	2.076	2.215	2.352	2.485	2.614	2.736	2.85		
0.9	1.816	1.948	2.084	2.224	2.362	2.498	2.632	2.757	2.88	2.99	
1.	1.818	1.954	2.093	2.231	2.372	2.51	2.646	2.776	2.903	3.02	3.131

Table 8: Exact values for the dividends of the Gamma distribution, Model A

$b\backslash x$	0	0.1	0.2	0.3	0.4	0.5	0.6	0.7	0.8	0.9	1.
0	0.245										
0.1	0.245	0.256									
0.2	0.246	0.257	0.267								
0.3	0.248	0.259	0.27	0.279							
0.4	0.251	0.262	0.274	0.283	0.291						
0.5	0.254	0.266	0.278	0.289	0.297	0.303					
0.6	0.258	0.27	0.283	0.294	0.304	0.312	0.316				
0.7	0.262	0.275	0.288	0.3	0.311	0.32	0.327	0.33			
0.8	0.266	0.28	0.294	0.307	0.319	0.329	0.337	0.343	0.346		
0.9	0.271	0.286	0.3	0.314	0.327	0.338	0.348	0.355	0.36	0.362	
1.	0.276	0.291	0.306	0.321	0.334	0.347	0.357	0.366	0.373	0.378	0.38

Table 9: Exact values for the survival probability of the Gamma distribution, Model B

$b\backslash x$	0	0.1	0.2	0.3	0.4	0.5	0.6	0.7	0.8	0.9	1.
0	1.096										
0.1	1.096	1.189									
0.2	1.092	1.186	1.286								
0.3	1.088	1.182	1.281	1.384							
0.4	1.082	1.176	1.276	1.377	1.481						
0.5	1.075	1.168	1.266	1.369	1.472	1.577					
0.6	1.064	1.157	1.256	1.357	1.461	1.566	1.671				
0.7	1.053	1.146	1.243	1.343	1.447	1.551	1.655	1.762			
0.8	1.039	1.132	1.228	1.327	1.43	1.535	1.64	1.745	1.85		
0.9	1.024	1.115	1.21	1.309	1.411	1.514	1.619	1.724	1.829	1.935	
1.	1.006	1.095	1.19	1.289	1.388	1.49	1.594	1.699	1.804	1.909	2.014

Table 10: Exact values for the dividends of the Gamma distribution, Model B

References

[1] J. Aczél. *Vorlesungen über Funktionalgleichungen und ihre Anwendungen.* Birkhäuser, Basel, 1960.

[2] H. Albrecher and R. Kainhofer. Risk theory with a non-linear dividend barrier. *Computing*, 2002. To appear.

[3] H. Albrecher, R. Kainhofer, and R. Tichy. Simulation methods in ruin models with non-linear dividend barriers. *Math. Comput. Simulation*, 2002. To appear.

[4] H. Albrecher and R. Tichy. On the convergence of a solution procedure for a risk model with gamma-distributed claims. *Schweiz. Aktuarver. Mitt.*, 2:115–127, 2000.

[5] S. Asmussen. *Ruin probabilities.* World Scientific, Singapore, 2000.

[6] S. Asmussen and K. Binswanger. Simulation of ruin probabilities for subexponential claims. *ASTIN Bull.*, 27(2):297–318, 1997.

[7] P. Bratley, B. L. Fox, and H. Niederreiter. Implementation and tests of low discrepancy sequences. *ACM Trans. Model. Comp. Simul.*, 2:195–213, 1992.

[8] H. Bühlmann. *Mathematical Methods in Risk Theory.* Springer, New York, 1970.

[9] R. Caflisch. Monte Carlo and Quasi-Monte Carlo methods. *Acta Numerica*, pages 1–46, 1998.

[10] F. De Vylder. *Advanced risk theory.* Editions de l'universite de Bruxelles, Bruxelles, 1996.

[11] F. Delbaen and J. Haezendonck. Classical risk theory in an economic environment. *Insurance: Mathematics and Economics*, 6:85–116, 1987.

[12] M. Drmota and R. Tichy. *Sequences, Discrepancies and Applications*, volume 1651 of *Lecture Notes in Mathematics.* Springer, New York, Berlin, Heidelberg, Tokyo, 1997.

[13] H. Faure. Discrépance de suites associées à un système de numération (en dimension un). *Bull. Soc. Math. France*, 109:143–182, 1981.

[14] H. U. Gerber. Martingales in risk theory. *Mitteilungen der Schweizer Vereinigung der Versicherungsmathematiker*, pages 205–216, 1973.

[15] H. U. Gerber. The dilemma between dividends and safety and a generalization of the Lundberg-Cramér formulas. *Scandinavian Actuarial Journal*, pages 46–57, 1974.

[16] H. U. Gerber. *An Introduction to Mathematical Risk Theory.* Huebner Foundation Monograph 8, Homewood, Ill, 1979.

[17] H. U. Gerber. On the probability of ruin in the presence of a linear dividend barrier. *Scandinavian Actuarial Journal*, pages 105–115, 1981.

[18] J. H. Halton. On the efficiency of certain quasi-random sequences of points in evaluating multidimensional integrals. *Numer. Math.*, 2:84–90, 1960.

[19] L. Heersink. Ruinmodelle mit linearen und nichtlinearen Dividendenschranken. Diplomarbeit, TU-Graz, Graz, Austria, 2001.

[20] H. Niederreiter. *Random Number Generation and Quasi-Monte Carlo Methods.* Society for industrial and applied mathematics, Philadelphia, Pennsylvania, 1992.

[21] J. Paulsen and H. Gjessing. Optimal choice of dividend barriers for a risk process with stochastic return on investments. *Insurance Math. Econom.*, 20:215–223, 1997.

[22] W. H. Press, S. A. Teukolsky, W. T. Vetterling, and B. P. Flannery. *Numerical Recipes in C.* Cambridge University Press, Cambridge, 1992.

[23] I. Radovic, M. Sobol', and R. F. Tichy. Quasi-monte carlo sequences for numerical integration: Comparison of different low discrepancy sequences. *Monte Carlo Methods and Applications*, 2(1):1–14, 1996.

[24] T. Siegl and R. Tichy. Lösungsmethoden eines Risikomodells bei exponentiell fallender Schadensverteilung. *Schweiz. Aktuarver.Mitt.*, 1:85–118, 1996.

[25] I. M. Sobol'. On the distribution of points in a cube and the approximate evaluation of integrals. *USSR Comput. Math. Math. Phys.*, 7:86–112, 1967.

[26] O. Thorin. Probabilities of ruin. *Scandinavian Actuarial Journal*, pages 65–102, 1982.

[27] R. F. Tichy. Über eine zahlentheoretische Methode zur numerischen Integration und zur Behandlung von Integralgleichungen. *Sitzungsberichte der Österreichischen Akademie der Wissenschaften*, 193, 1984.

H. Albrecher, R. Kainhofer and R. Tichy
Department of Mathematics
Graz University of Technology
Steyrergasse 30
8010 Graz
Austria